Near-threshold behavior of the 2*p*-electron excitation in Mg-Mg, Al-Al, and Si-Si symmetric collisions

N. Mandarino, P. Zoccali, A. Oliva, M. Camarca, A. Bonanno, and F. Xu
Dipartimento di Fisica, Università della Calabria, 87036 Arcavacata di Rende, Cosenza, Italy
(Received 11 May 1993)

Target *LMM* atomic Auger electron emission has been studied by low-energy ion bombardment on light-element surfaces. Our results show that the threshold energies for Mg, Al, and Si 2*p* core electron excitation are the same for impact of Ar^+, Kr^+, and Xe^+ projectiles but are substantially lower for Ne^+. A sensitive dependence of the energy onset on the ion incidence angle has also been observed. The intensity behavior in the near-threshold energy range is in excellent agreement with simple kinematic calculations using a binary-collision model and by taking into account only the first target-target symmetric encounters.

PACS number(s): 32.80.Hd, 79.20.Rf, 79.20.Nc, 34.50.Fa

I. INTRODUCTION

Studies of Auger-electron emission induced by ion bombardment on light-element solid targets have attracted great interest in recent years both because the incomparably higher material density relative to the gas targets allows the use of near-threshold impact energies and because they can provide interesting insight into the peculiarities of ion-solid interactions [1–3]. The core electron excitation mechanism has long been interpreted with the molecular-orbital (MO) model [4,5], according to which a transient molecule is formed during a collision between two atoms, and if the minimum internuclear distance is smaller than a critical value R_{th} then some MO's can cross over each other, leading to the promotion of one or two core electrons into high-lying empty levels. The experimental determination of the threshold energy E_{th} corresponding to such R_{th} is thus one of the essential problems concerning collisional core electron excitation. In fact, a large number of computer-simulation studies reported in literature used very different R_{th} values in combination with different choices of other physical parameters and apparently all of them gave quite good agreement with a particular series of experimental data [6–10]. However, Hou, Benazeth, and Benazeth [9] recently showed that, with other parameters fixed, the Auger yield depends sensitively on R_{th} (or E_{th}). Therefore the knowledge of such a critical parameter is of fundamental importance if any useful information is to be extracted from this kind of comparison.

Many attempts to obtain threshold energies from Auger intensity measurements have been made in the last 15 years. Vrakking and Kroes [11] found E_{th} values of 400, 750, and 1380 eV for Mg, Al, and Si, respectively. Fan, Yu, and Chen [12] reported much lower values for various compounds of light metals (MgO, Al_2O_3, SiO_2). Baragiola, Alonso, and Raiti [13] obtained a threshold energy of 0.9 keV for Al-Al. Valeri and Tonini [14] measured an E_{th} of about 1 keV for Si-Si. However, as pointed out first by Ferrante and Pepper [15] and recently demonstrated by Baragiola, Nair, and Madey [16], even a small contamination of doubly charged ions (with a double energy) in the primary beam can significantly alter the experimentally determined E_{th} values. This raises serious doubts on the reliability of the early measurements.

In this paper, we present a detailed experimental study on the reexamination of the threshold-energy problem by bombarding Mg, Al, and Si samples with different noble-gas ions at different primary energies. We have carefully measured the actual projectile-ion kinetic energy, definitely eliminated the double charges, and reduced the experimental uncertainty to less than 25 eV for each series of measurements. Our values are much lower than those commonly used in computer-simulation studies and provide an experimental base for the choice of E_{th} or R_{th}. Further, we also carried out a systematic kinematic calculation to better interpret the Auger intensity behavior in the near-threshold energy range and to provide interesting insight into the role played by the different projectiles in determining the efficiency of the secondary symmetric collisions.

II. EXPERIMENT

The experiment was performed in an UHV chamber with a base pressure in the mid-10^{-10} Torr range. During measurements it rose to 1×10^{-8} Torr. Noble-gas ions (Ne^+, Ar^+, Kr^+, and Xe^+), supplied by a differentially pumped Atomika ion source, were used as projectiles. For each gas employed the discharge voltage was set at several volts below the second ionization potential to ensure the total absence of the doubly charged ions. The ion accelerating voltage was directly measured using either a voltmeter or a calibrated high-voltage probe. Because of the very small aperture (2 mm) of the ionization chamber, the gas discharge voltage and the filament voltage had a negligible influence on the projectile-ion kinetic energy whose total uncertainty was less than ±5 eV.

The ion-current density had a Gaussian profile in both

1050-2947/93/48(4)/2828(4)/$06.00

horizontal and vertical directions, as characterized with a movable Faraday cup situated at the position of the sample surface. To avoid the change in the analyzer detection area due to the variation of either the ion incidence angle or the beam size (0.6–1.2 mm) and to reduce the topography problems, the ion beam was set to raster a large constant sample surface of 4×4 mm^2 (linear ramps with frequencies of 10^3 and 10^2 Hz) and the measured Auger yield was normalized to both maximum current density and the beam widths.

Mg, Al, and Si samples were mounted on a sample manipulator and its rotation allowed the change of the ion incidence angle relative to the surface normal. The emitted Auger electrons were collected by a hemispherical energy analyzer situated at a fixed angle of 70° with respect to the ion-beam direction. The analyzer semiacceptance angle was 25° and a constant pass energy of 100 eV was used to ensure an adequate instrument sensitivity level. Because of the high stability of the ion source, spectra were often recorded over a long time period (~ 12 h) to yield a reasonable statistics.

III. RESULTS AND DISCUSSION

In Fig. 1 we present four sets of Al Auger-electron spectra obtained by Ar^+ ion bombardment on Al at incidence angles of $\theta_i = 0°$, 30°, 50°, and 70° relative to the surface normal for various primary-ion energies E_p. These spectra clearly demonstrate the very existence of the energy threshold for the collisional excitation processes and show a sensitive dependence of the energy onset for the observation of the atomic *LMM* signals on the ion incidence angle. In fact, at the threshold, two colliding target atoms can reach the critical minimal approach distance only in a head-on encounter and the impinging target atom can acquire a maximum kinetic energy from the projectile atom only in a previous asymmetric collision which is also head-on. However, such a sequence of encounters cannot produce the direct ejection of the excited particle from the sample surface if the incidence angle is not $\theta_i = 90°$. Therefore, in at least one of the two collisions, a deviation should occur. The larger the deviation, the larger the impact energy should be in order to reach the critical minimal approach distance. On the other hand, though the onset of the bulk *LVV* signal (*V* denotes the valence band) should be independent on θ_i, its large spectral width renders the separation from the secondary-electron background very difficult, as demonstrated by the curves shown in Fig. 1. Thus the best practical way to determine the threshold is to monitor the atomic Auger yield using grazing incidence angles.

In Fig. 2 we show Mg and Si *LMM* Auger-electron

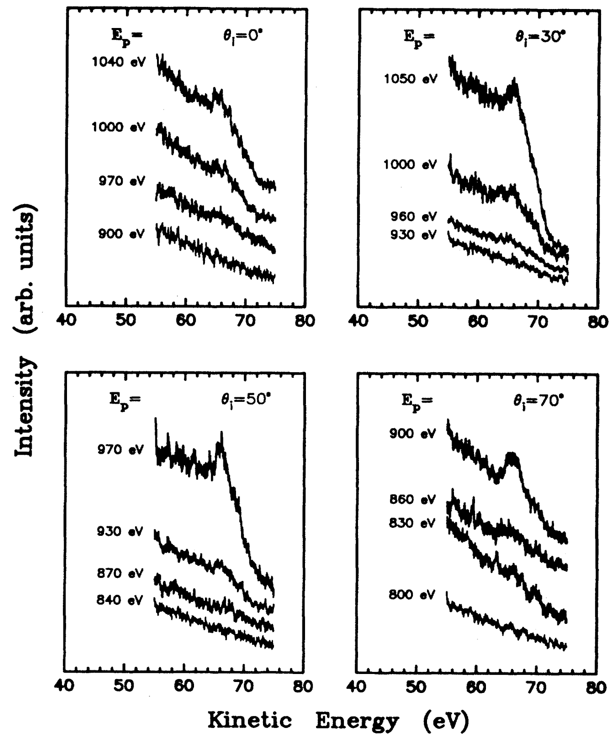

FIG. 1. Al *L*-shell Auger-electron spectra taken for Ar^+ ion bombardment on Al at four different incidence angles for various primary-ion energies.

spectra obtained by bombardment of Ar^+ ions with primary energies close to the threshold values and at an incidence angle of 70°. As in the case of Al, these spectra again clearly show the possibility of determining the critical energy for core electron excitation with a relatively small uncertainty. The experimentally observed values γE_{th}^{obs} for $\theta_i = 70°$ are given in Table I for various systems studied. They were calculated as

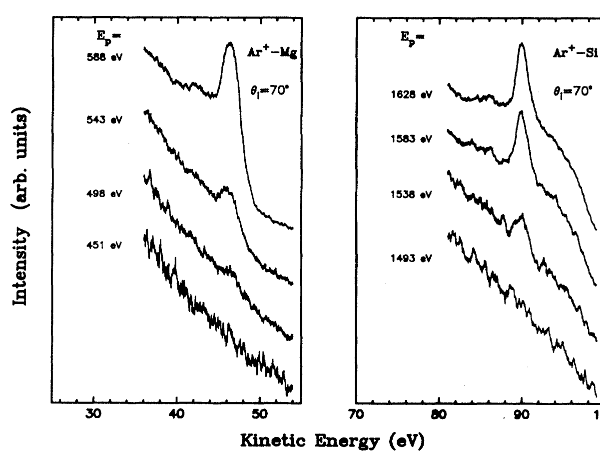

FIG. 2. Target *L*-shell Auger-electron spectra taken for Ar^+ ion bombardment on Mg and Si surfaces for primary energies close to the threshold values for secondary symmetric collisions. The incidence angle is 70° relative to the surface normal.

TABLE I. Experimental threshold energies γE_{th}^{obs} (eV) observed at $\theta_i = 70°$.

	Ne^+	Ar^+	Kr^+	Xe^+
Mg	271±24	447±24	457±18	417±16
Al	450±24	784±17	816±19	
Si	1386±25	1469±24	1480±19	1431±16

$$\gamma E_{\text{th}}^{\text{obs}}=\tfrac{1}{2}\gamma(E_1+E_2)\pm\gamma\sqrt{\tfrac{1}{4}(E_1-E_2)^2+\Delta E_1^2+\Delta E_2^2}\ ,$$

where E_1 and E_2 are the primary-ion energies of the two spectra for which it was possible to unambiguously establish the presence or the absence of the *LMM* signals and ΔE_1 and ΔE_2 are the uncertainties in the ion kinetic energies. The very similar $\gamma E_{\text{th}}^{\text{obs}}$ values for Ar^+, Kr^+, and Xe^+ projectiles provide convincing evidence that they are indeed relative to the symmetric target-target collisions.

We note that the Al *LMM* Auger peak partially overlaps with the Xe 4*d* autoionization features (their existence was checked in the Xe^+-Mg system). Though the very small contribution of the latter does not alter the evaluation of the Al intensity at energies well above the threshold, it renders very difficult an accurate determination of $E_{\text{th}}^{\text{obs}}$ for Al-Al in the case of Xe^+-Al. The much lower threshold values obtained for Ne^+ than those for other projectiles, already noticed by Baragiola, Alonso, and Raiti previously [13] for Ne^+-Al, is a clear indication of the target-atom excitation in slightly asymmetric Ne-Mg, Ne-Al, and possibly also Ne-Si collisions. These $\gamma E_{\text{th}}^{\text{obs}}$ are related to the threshold energies for the Ne double 2*p* vacancy creation in such encounters. A detailed discussion on the inner excitation of the heavier partner will be presented in a separate paper [17].

As we already pointed out above, the $\gamma E_{\text{th}}^{\text{obs}}$ values measured at $\theta_i=70°$ represent only the upper limit of the true excitation threshold E_{th}, which can be estimated using the formalism of the classical mechanics for a binary collision. However, such corrections, obtained with the kinematic calculations discussed in detail below, amount to only a few eV for Mg, Al, and Si and do not affect the experimental errors.

It is interesting to note that our threshold energies are larger than the values previously reported in the literature [11,12,14]. The main reason is the possible contamination of the doubly charged ions (with double energy) in these early works. Nevertheless, they are still much smaller than the values predicted by the MO correlation diagrams (1.1 ± 0.1, 1.7 ± 0.2, and 2.6 ± 0.3 keV for Mg-Mg, Al-Al, and Si-Si, respectively; see Ref. [18]). Even more surprisingly, for the case of Al, the E_{th} is significantly lower than the value (1.6 keV) obtained by Hou, Benazeth, and Benazeth [9] by fitting the experimental Auger yield for 5-keV Ar^+-Al with computer simulations. Such very large discrepancies may be an indication of the large inaccuracy of the adiabatic MO calculation scheme and the inadequate choice of the other physical parameters in the simulations and strongly suggests that much more effort is needed for the understanding of the collisional excitation at impact energies close to the threshold values.

In Fig. 3 we plot the intensities of the main atomic *LMM* Auger peaks of Mg, Al, and Si as a function of the maximum transferred energy γE_p for different projectile ions. The slight but systematic divergence of these curves, noticed previously [13], reflects the divergence of the cross sections for the *p*-*t* collisions, precursor of the secondary *t*-*t* collisions.

To better understand this behavior, we calculated the differential yield dY/db_1 for the ejection of an excited *t* particle from the surface in a second *t*-*t* symmetric encounter as a function of the impact parameter b_1 of the first *p*-*t* asymmetric elastic collision for $\theta_i=70°$. In doing so, we first varied b_1 from 0 to $a/2$ (a is the average distance between two target atoms) with a constant step db_1 and for each interval b_1 and b_1+db_1 calculated the cross section σ_1 that the target recoil is scattered into a solid angle of $\sin\theta\, d\theta\, d\phi$ with a transferred kinetic energy between E_t and E_t+dE_t. For each generatrix on the cones,

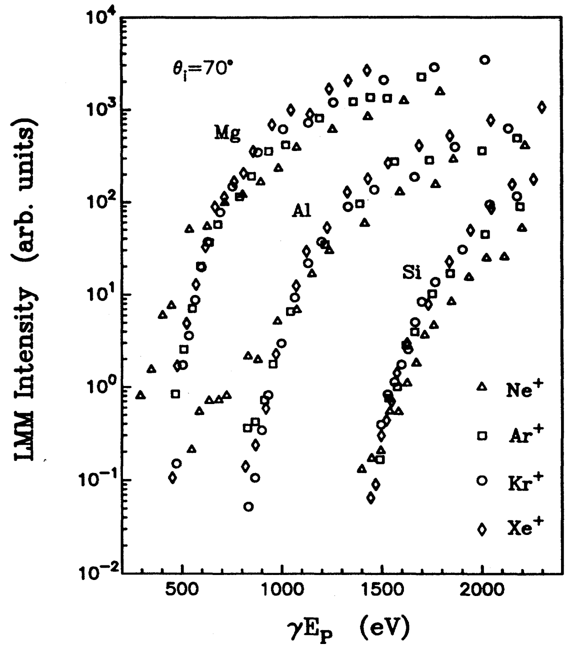

FIG. 3. Mg, Al, and Si atomic *LMM* Auger intensities as a function of the maximum transferred kinetic energy in a primary asymmetric collision. The ion incidence angle is $\theta_i=70°$ relative to the surface normal.

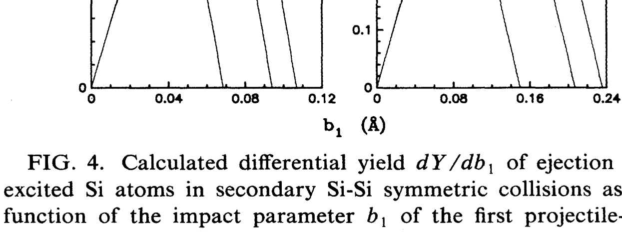

FIG. 4. Calculated differential yield dY/db_1 of ejection of excited Si atoms in secondary Si-Si symmetric collisions as a function of the impact parameter b_1 of the first projectile-Si asymmetric elastic collision for two fixed γE_p values. The Moliére potential was used and R_{th} was chosen to be 0.495 Å, determined from our experimental threshold energy for Si-Si.

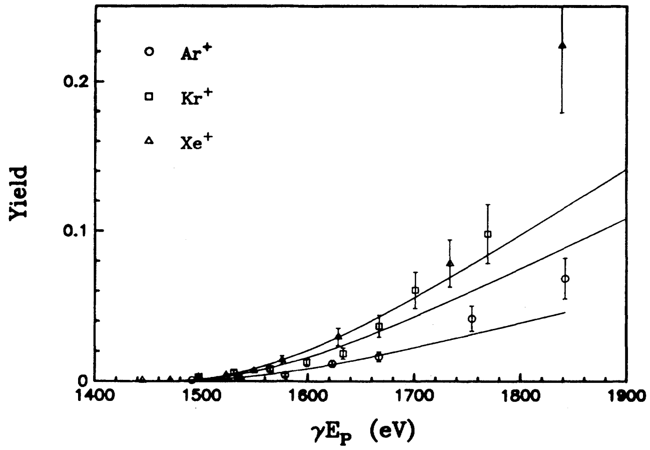

FIG. 5. Comparison between the calculated total Auger yield, obtained by integrating the curves of Fig. 4, and the properly scaled experimental Si *LMM* intensity.

or parts of the cones, directed inward the sample, we then calculated the cross section $\sigma_2 = \sigma_2\ (\theta,\phi,E_t)$ for the ejection of an excited particle out of the surface in a secondary symmetric collision in which either projectile or recoil particles can be excited with an equal probability of 0.5 if the minimal approach distance is smaller than R_{th}. The sample was assumed to be amorphous, i.e., the impact parameter in the secondary t-t collisions was again scanned equally probably. The integration over all σ_2 then gives the differential yield dY/db_1. The Moliére approximation to the Thomas-Fermi potential and the Firsov screening length were used in these calculations. In doing the normalization we also took into account that the area of sight is $a^2\cos\theta_i$ for an incoming noble-gas ion. Some typical examples are plotted in Fig. 4 for the cases of Ar^+-Si, Kr^+-Si, and Xe^+-Si for two different γE_p. These curves show that the heavier the projectile, the larger the critical impact parameter $b_{1,\mathrm{th}}$ and the larger the maximum differential yield.

The total yield, representing the number of the ejected target atoms per incoming ion and obtained by integration over all b_1, is presented in Fig. 5 as a function of the primary energy for Xe^+-Si, Kr^+-Si, and Ar^+-Si, together with the experimental Auger intensities, properly scaled for a constant factor. The excellent agreement at low γE_p then clearly confirms the validity of the simple binary-collision model and provides an interesting interpretation of the observed systematic divergence of the Auger yield. The gradual deviation of the experimental values at high γE_p from that predicted by our model calculations is an indication of the increasing importance of the cascade symmetric collisions in contributing to the target-atom excitation and their ejection from the surface.

IV. CONCLUSIONS

In summary, we have carefully determined the experimental threshold energies for $2p$ inner-electron excitation in symmetric Mg-Mg, Al-Al, and Si-Si collisions. Our results clearly show that the observed energy onset for atomic *LMM* Auger signals depends sensitively on the ion incidence angle, that the binary-collision model is indeed quite a good approximation for the description of collisional excitation in the solids, and that Ar^+, Kr^+, and Xe^+ projectiles yield the same threshold energies but Ne^+ impact results in lower-energy onset values due to the excitation of the heavier partner in asymmetric collisions. The threshold energies found in this study differ substantially from those predicted by molecular-orbital correlation diagrams and from those commonly used in literature for computer-simulation studies. Our kinematic calculations provide further interesting insight into the observed systematic divergence of the intensity behavior for different projectiles.

ACKNOWLEDGMENTS

We are indebted to V. Fabio and E. Li Preti for technical assistance. The group is also affiliated with the Consorzio Interuniversitario Nazionale per la Fisica della Materia.

[1] S. Valeri, Surf. Sci. Rep. **17**, 85 (1993).
[2] J. A. D. Matthew, Phys. Scr. **T6**, 79 (1983).
[3] F. Xu and A. Bonanno, Surf. Sci. **273**, L414 (1992).
[4] U. Fano and W. Lichten, Phys. Rev. Lett. **14**, 627 (1965).
[5] M. Barat and W. Lichten, Phys. Rev. A **6**, 211 (1972).
[6] T. D. Andreadis, J. Fine, and J. A. D. Matthew, Nucl. Instrum. Methods **209/210**, 495 (1983).
[7] C. Benazeth, N. Benazeth, and M. Hou, Surf. Sci. **151**, L137 (1985).
[8] O. Grizzi and R. A. Baragiola, Phys. Rev. A **35**, 135 (1987).
[9] M. Hou, C. Benazeth, and N. Benazeth, Phys. Rev. A **36**, 591 (1987).
[10] M. Shapiro and J. Fine, Nucl. Instrum. Methods B **44**, 43 (1989).
[11] J. J. Vrakking and A. Kroes, Surf. Sci. **84**, 153 (1979).
[12] C. Fan, Z. Yu, and X. Chen, J. Vac. Sci. Technol. A **5**, 1206 (1987).
[13] R. A. Baragiola, E. V. Alonso, and H. J. L. Raiti, Phys. Rev. A **25**, 1969 (1982).
[14] S. Valeri and R. Tonini, Surf. Sci. **220**, 407 (1989).
[15] J. Ferrante and S. V. Pepper, Surf. Sci. **57**, 613 (1976).
[16] R. A. Baragiola, L. Nair, and T. E. Madey, Nucl. Instrum. Methods B **58**, 322 (1991).
[17] F. Xu, N. Mandarino, P. Zoccali, A. Oliva, M. Camarca, and A. Bonanno Nucl. Instrum. Methods B (to be published).
[18] F. Xu, F. Ascione, N. Mandarino, P. Zoccali, P. Calaminici, A. Oliva, A. Bonanno, and N. Russo, Phys. Rev. B (to be published).